

# Late Quaternary thrusting in the southern margin of the Chaiwopu Basin, northern Chinese Tian Shan foreland

Lichen Pang<sup>1</sup> | Lu Cheng<sup>1</sup> | Honghua Lu<sup>1,2</sup> | Xue Guan<sup>1</sup> | Dengyun Wu<sup>3</sup> | Xiangmin Zheng<sup>1</sup>

<sup>1</sup>Key Laboratory of Geographic Information Science of Ministry of Education, School of Geographic Sciences, East China Normal University, Shanghai, China

<sup>2</sup>Institute of Eco-Chongming (IEC), East China Normal University, Shanghai, China

<sup>3</sup>Institute of Geology, China Earthquake Administration, Beijing, China

## Correspondence

Honghua Lu, No. 500 Dongchuan Rd., Minhang Dist., School of Geographic Sciences, East China Normal University, Shanghai 200241, China.  
Email: hhlv@geo.ecnu.edu.cn

## Funding information

Fundamental Research Funds for the Central Universities; National Natural Science Foundation of China, Grant/Award Number: 41371031 and 41771013

## Abstract

Thrusting and the associated folding are crucial geological processes accommodating the crustal shortening in a foreland setting. This work focuses on the late Quaternary thrusting of the Banfanggou fault (BF) in the southern Chaiwopu Basin, northern Chinese Tian Shan foreland. The outcrops at the Urumqi River in the western part of the southern margin of the basin show that the BF, dipping south with angle of 60–80°, has thrust the Neogene mudstone onto the Quaternary gravels and has displaced the terrace surfaces. In contrast, the eastern segment of the BF exists as a blind thrust fault. By using the geomorphic surface (river terrace and alluvial fan) as the reference, the average rate of vertical slip on the western segment of the BF over the past ~12 ka is estimated to ~1.7 mm/year, and the estimated rate at the eastern segment of the fault is ~1.0–1.3 mm/year. Despite of the uncertainties of the rates deriving from the vertical offsets and the geomorphic ages, the resultant vertical slip rates might imply relatively high seismic risk in the southern Chaiwopu Basin.

## KEYWORDS

Late Quaternary, slip rate, the Banfanggou fault, the Chaiwopu Basin, the Tian Shan

## HIGHLIGHTS

- The geometry of the Banfanggou fault (BF) in the southern Chaiwopu Basin is characterized
- The eastern segment of the BF exists as a blind thrust fault
- The vertical slip rate on the BF is estimated to likely >1 mm/year

## 1 | INTRODUCTION

The Tian Shan range is a typical active orogenic belt in the inland of Asian. In response to the Early Cenozoic India–Asia collision (Avouac & Tapponnier, 1993; Najman et al., 2001), the Tian Shan has been tectonically reactivated and intensively uplifted by absorbing the north-south crustal shortening (Deng et al., 2000; Zhang, 2004). As the result of propagation of the range into its foreland basins, several fold-and-thrust belts approximately parallel to the strike

of the range have been formed (Deng et al., 2000; Lu et al., 2015, 2019; Figure 1a). These piedmont structural belts have documented the history of deformation and propagation of the range and, thus, provide us a natural laboratory to understand the mechanism of the Cenozoic deformation of the Tian Shan.

The Chaiwopu Basin is located in the easternmost part of the northern Chinese Tian Shan foreland (Figure 1b). In the southern margin of the basin, two thrust faults control the local topography and tectonics. One is the Junggar Frontal Thrust Fault (JFTF), which separates the Nan Shan (the northern Tian Shan) to the south from the Chaiwopu Basin to the north. The other is the Banfanggou fault (BF), a branch of the JFTF, which has controlled growth and deformation of the Saerqiao anticline (Lu et al., 2015; Figure 1c,d). These structures consist of a typical piedmont 'thin skin' structural system (Liu & Chen, 2002; Lu et al., 2015), and have been proposed to be primarily responsible for the seismicity in the southern Chaiwopu Basin (Deng et al., 2000). During the past two decades, a lot of studies

have been conducted on the fold-and-thrust belts in the western part of the northern Tian Shan foreland, including the history of anticlinal growth and deformation (e.g. Avouac et al., 1993; Burchfiel et al., 1999; Charreau et al., 2008; Fu et al., 2017; Gong et al., 2015; Lu et al., 2019; Qiu et al., 2019; Scharer et al., 2006; Wei et al., 2019), fluvial geomorphological evolution (e.g. Gong et al., 2014; Li et al., 2012; Lu et al., 2010, 2014, 2017) and geodetic investigations (e.g. Charreau et al., 2018; Yang et al., 2008). In contrast, few studies (e.g. Lu et al., 2015) have been concentrated in the eastern part of the foreland, i.e. the Chaiwopu Basin. The geometry of the BF and its activation during the late Quaternary still need further investigation.

In this study, we focus on the BF in the southern margin of the Chaiwopu Basin (Figure 1c), where deformed geomorphic surfaces have documented the history of the late Quaternary thrusting of this fault. We define the geometry of the BF by characterizing the sedimentary strata exposed in outcrops. The geomorphic surface (river terrace and alluvial fan) is used as the reference to characterize the recent deformation of the fault. By morphometry, the vertical offset of the BF recorded by the reference is determined. When combined with the abandonment age of the geomorphic marker constrained by optically stimulated luminescence (OSL) dating, the average rate of vertical slip on the BF is estimated. The main aim of this study is to reveal the geometry of the BF and its activation, and further to understand the spatial pattern of vertical slip rate in the north piedmont of the Chinese Tian Shan, a typical active orogenic belt with high seismicity in Central Asian.

## 2 | GENERAL SETTINGS

The EW-trending Tian Shan has experienced a complex geological history during the Palaeozoic (Reigber et al., 2001; Tapponnier et al., 2001). In response to the Cenozoic India-Asia collision, the Tian Shan has been reactivated and intensively uplifted (Deng et al., 2000). As a result, a series of EW-striking fold-and-thrust belts have been formed in both the southern and northern foreland basins of the range (Burchfiel et al., 1999; Deng et al., 2000; Figure 1a). In the easternmost part of the northern Chinese Tian Shan foreland is located in the Chaiwopu Basin. Thrusting on the BF has caused growth and propagation of the Saerqiaoke anticline in the southern margin of the basin (Lu et al., 2015; Figure 1d). Our previous magnetostratigraphic study has constrained the initiation of anticlinal growth at about 6 Ma (Lu et al., 2015), implying the synchronous thrusting on the BF. Stratigraphically, the Chaiwopu Basin has been filled with the Palaeogene-Neogene to Quaternary sediments. The Palaeogene-Neogene strata comprise the Donggou Group (Palaeocene-Eocene), the Manas (Oligocene), the Qianshan (Miocene) and the Changjihe (Pliocene) Formations (Lu et al., 2015; Zhou et al., 2002). Lithologically, these Palaeogene-Neogene strata are fluvial-lacustrine mudstone, sandstone and conglomerates (Lu et al., 2015). The basement rocks of the basin are composed of the Permian to Triassic strata (Gao, 2004). As the result of tilting, thrusting and folding, the basement rocks and the Palaeogene-Neogene

strata are exposed on both the southern and northern margins of the Chaiwopu Basin (Gao, 2004; Lu et al., 2015).

Several river systems (i.e. the Urumqi River, the Banfanggou Creek, the Shuixi Creek, the Xiaodong Creek and the Wushencheng Creek) flow across the Nan Shan and incise into the southern Chaiwopu Basin (Figure 1c). The Urumqi River has the largest catchment area that originates from the Glacier NO.1 flowing from the Tangger Peak in the axial part of the range. The annual precipitation in the Chaiwopu Basin is about 100–200 mm (Gao, 2004). Thus, the fluvial water supply of the Urumqi River depends mainly on the glacier melt. The river flows into the lowland southern Chaiwopu Basin and have developed three stages of the late Quaternary alluvial fan (Lu et al., 2014). The other four creeks display the similar fluvial geomorphological framework at the mountain front (Figure 1c), whereas they have smaller catchment areas and, thus, less discharge in comparison with the Urumqi River.

## 3 | ALLUVIAL SEQUENCES

In order to characterize the deformation of the Banfanggou fault using the geomorphic marker, the alluvial sequences in the southern margin of the Chaiwopu Basin are first classified. The geomorphic ages are constrained by optically stimulated luminescence (OSL) dating method. The details about the methodology are shown in Data S1 in Supporting Information uploaded online. Based on the new outcomes and our previous work (Lu et al., 2014), three episodes of alluvial fan development in the southern Chaiwopu Basin are defined; they are designated as fans  $F_1$ ,  $F_2$  and  $F_3$  (progressively younger in abandonment age) in this work.

Fan  $F_1$  is widely distributed at the mountain front of the Urumqi River (Figure 1c). The alluviums of fan  $F_1$  are mainly comprised of gray gravels, and the maximum thickness at the fan head has been estimated to ~ 400 m (Zhou et al., 2002). Since the abandonment of fan  $F_1$  at about 0.55 Ma (Lu et al., 2014), nine terraces ( $T_1$  to  $T_9$ , progressively higher in elevation) have successively formed owing to subsequent river incision (Lu et al., 2014; Zhou et al., 2002). Geomorphologically, terraces  $T_9$  and  $T_4$  correspond to fans  $F_1$  and  $F_2$  respectively. Among these nine terraces,  $T_7$ ,  $T_5$  and  $T_4$  are the best expressed fluvial features at the mountain front of the Urumqi River (see figure 4 of Lu et al., 2014). The characters of these three terraces have been described in our previous work (Lu et al., 2014), and this work focuses on their abandonment ages. By using electron spin resonance (ESR) dating on the terrace deposits, the abandonment age of terrace  $T_7$  has been constrained at ~255 ka (Lu et al., 2014). As for terrace  $T_5$ , an ESR sample taken from the layer of silt at the top of terrace gravels was dated to  $142 \pm 14$  ka (Lu et al., 2014). This age is obviously older than the OSL age of  $27.4 \pm 3.1$  ka of the sample taken from the base of loess covering the deposits of terrace  $T_5$  (Lu et al., 2016), likely implying that the loess has not accumulated immediately after terrace abandonment. Given the uncertainty of the dates, we do not determine the time interval between terrace abandonment and loess deposition. Better constraint on the

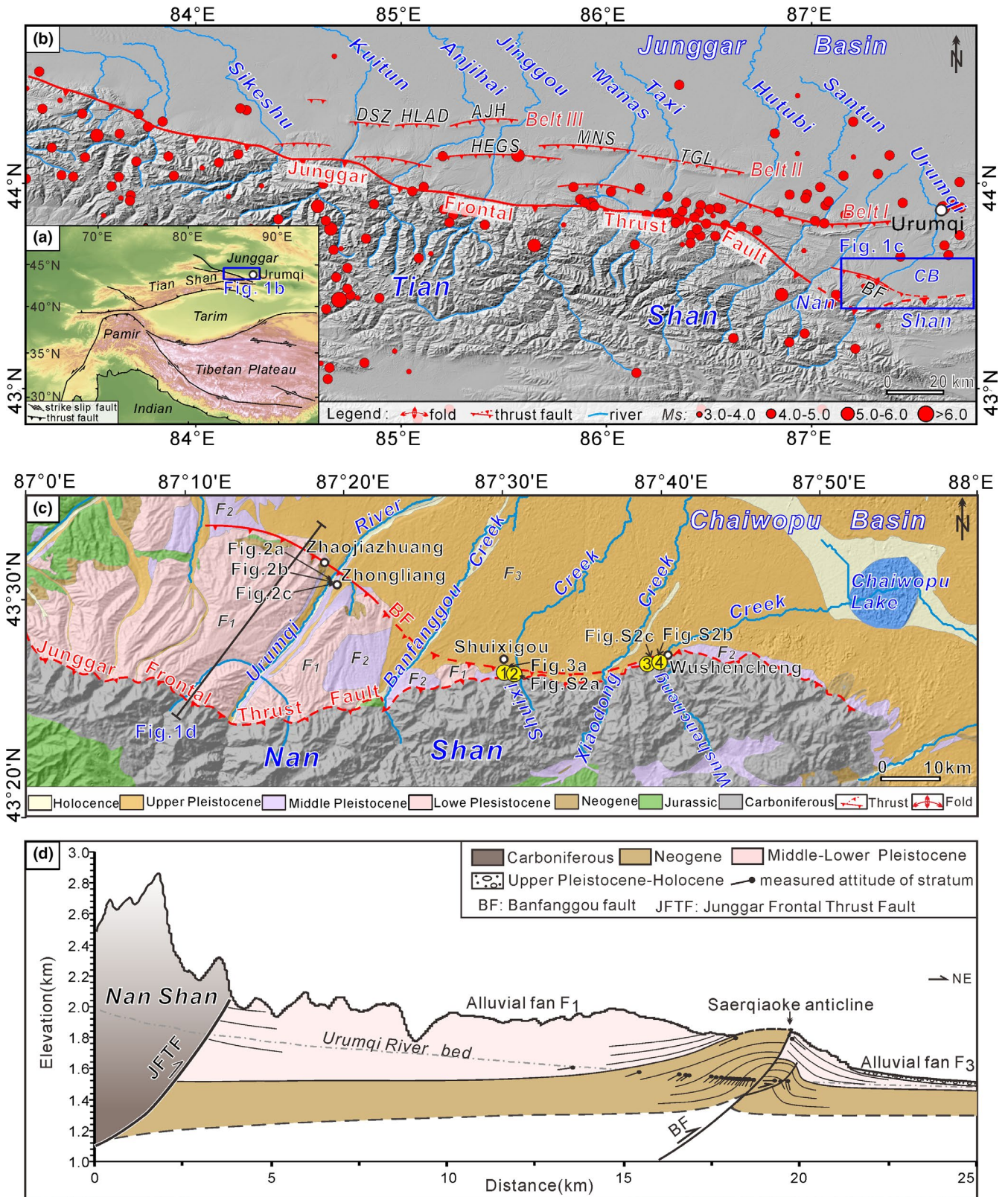


**FIGURE 1** (a) Map showing the topographic and tectonic patterns of the Tibetan Plateau and its surrounding region. (b) Tectonics and river systems in the northern Chinese Tian Shan foreland. Thrust faults in the fold-and-thrust Belt II: HEGS = Huoerguos fault, MNS = Manas fault, TGL = Tugulu fault; Belt III: DSZ = Dushanzi fault, HLAD = Halaande fault, AJH = Anjihai fault. BF = Banfanggou fault. CB = Chaiwopu Basin. The earthquake data are downloaded from the USGS: <https://earthquake.usgs.gov/earthquakes/>. (c) Map showing the stratigraphy and the alluvial sequences (alluvial fans F<sub>1</sub>, F<sub>2</sub> and F<sub>3</sub>) in the southern Chaiwopu Basin. Yellow circles with numbers are the OSL dating samples. (d) Geological section (after Lu et al., 2015) along the west bank of the Urumqi River displaying a typical thrust nappe that is mainly composed of the Junggar Frontal Thrust Fault (JFTF) and the BF. (For interpretation of the references to colour in this figure legend, the reader is referred to the web version of this article.) [Colour figure can be viewed at [wileyonlinelibrary.com](http://wileyonlinelibrary.com)]

abandonment of this terrace need further numerical dating on the terrace deposits. Until now, no numerical date on the abandonment age of terrace  $T_4$  is available. Based on the similarity of the Urumqi River terrace  $T_4$  with the 12-ka terraces of the other piedmont rivers in the northern Tian Shan foreland, the abandonment age of the Urumqi River terrace  $T_4$  has been estimated to be ~12 ka (Wu et al., 2020).

In relation to fan  $F_1$ , fan  $F_2$  is locally distributed where the four creeks (the Bangfanggou, Shuixi, Xiaodong and Wushencheng creeks) exit from the mountain range (Figure 1c). The field investigations show that the surface of fan  $F_2$  is relatively planar. Lithologically, the alluviums of fan  $F_2$  are similar to that of fan  $F_1$ . In comparison with fan  $F_1$ , the gullies on the surface of fan  $F_2$  have not incised too deeply and commonly have the length of tens of metres.

Fan  $F_3$  is widely and continuously distributed to the north of fans  $F_1$  and  $F_2$ , existing as an alluvial plain (Figure 1c). The alluviums of fan  $F_3$  are composed of black-gray gravel and sand, and its surface is under farming. According to the formation age of < 4 ka of the low terrace preserved in the river valley (Lu et al., 2014), fan  $F_3$  may have formed during the latest Pleistocene-Early Holocene.

## 4 | LATE QUATERNARY THRUSTING OF THE BANFANGGOU FAULT

### 4.1 | Geometry of the Banfanggou Fault

The geometry of the BF is revealed in outcrops at two sites, i.e. Zhongliang (Figure 2) and Shuixigou (Figure 3). At Zhongliang, the outcrops exposed on the west and east sides of the Urumqi River valley obviously show the geometry of the BF (Figure 2). Just near the riverbed on the west side of the river valley, the BF has the dip direction of  $211^\circ$  and the dip angle of  $83^\circ$  (Figure 2a). On the east side of the river valley where the elevation increases by about 50 m in comparison with the site of Figure 2a, the dip angle of the fault

is ~  $60\text{--}70^\circ$  and the dip direction is ~  $215^\circ$  (Figure 2b,c). As revealed in these above outcrops, the BF has thrust the Neogene mudstone over the Quaternary conglomerates (Figure 2), and has further deformed the young terraces (see Section 4.2.1).

In relation to the exposure of the BF at Zhongliang, the geometry of the BF at Shuixigou is not revealed very well, but it can be inferred from the changes in attitudes of strata and topography (Figure 3; Figure S2). In an outcrop from sand extraction at the edge of fan  $F_2$ , the exposed strata are composed of layers of gravels and sand with clear stratification, and the strata dip northward (Figure 3b). In the southern part of the outcrop, the strata dip gently at an angle of less than  $5^\circ$ . In its middle part, the dip angle increases to about  $12^\circ$ . The maximum dip angle ( $29^\circ$ ) is observed in the northern part of the outcrop (Figure 3b). This change in the attitude of strata is marked by an abrupt steepening of the topography between fans  $F_2$  and  $F_3$  (Figure 3a; Figure S2a). Given that original attitude of alluvium deposited along a mountain front is commonly characterized by a relatively gentle dip of a few degrees, the observed changes in attitude of strata of fan  $F_2$  (Figure 3b) and topography (Figure 3a; Figure S2a) at Shuixigou are interpreted as the result of thrusting of a blind fault, which should be the eastern segment of the BF (Figure 1c).

### 4.2 | The vertical slip rate of the Banfanggou Fault

#### 4.2.1 | Zhongliang

At Zhongliang, the faulted Urumqi River terraces have documented the history of deformation of the BF (Figure S3). The topographic profiles extracted from the digital elevation model (DEM) indicate that terraces  $T_7$ ,  $T_5$  and  $T_4$  have been significantly offset by the fault (Figure S3). In the footwall of the BF, terraces  $T_7$  and  $T_5$  have been buried due to accumulation of younger alluvial sediments (Figure S3). Thus, it is unlikely to quantitatively determine the cumulative vertical offsets of the BF since formation of terraces  $T_7$  and  $T_5$ . It is clear

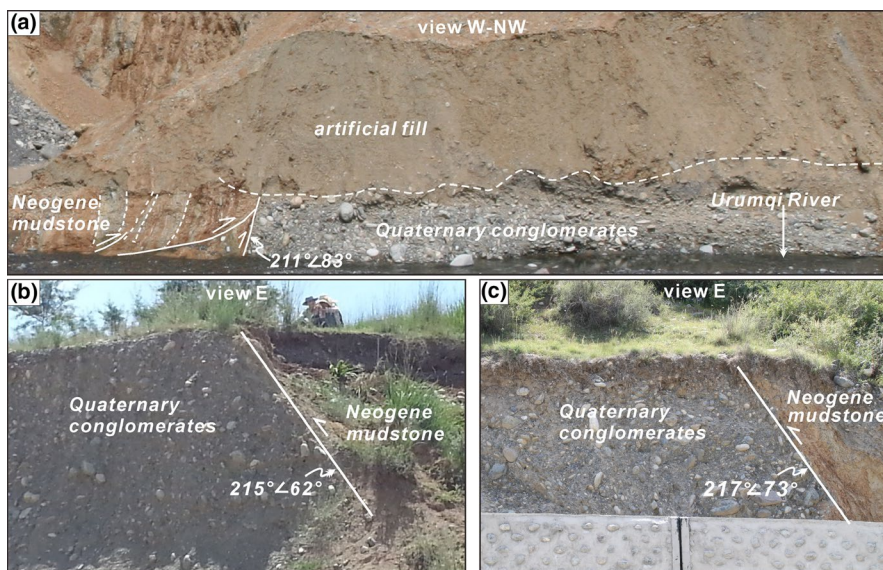


**FIGURE 2** Photos showing the geometry of the Banfanggou fault at Zhongliang village on the western and eastern bank of the Urumqi River valley. (For interpretation of the references to colour in this figure legend, the reader is referred to the web version of this article.) [Colour figure can be viewed at [wileyonlinelibrary.com](http://wileyonlinelibrary.com)]

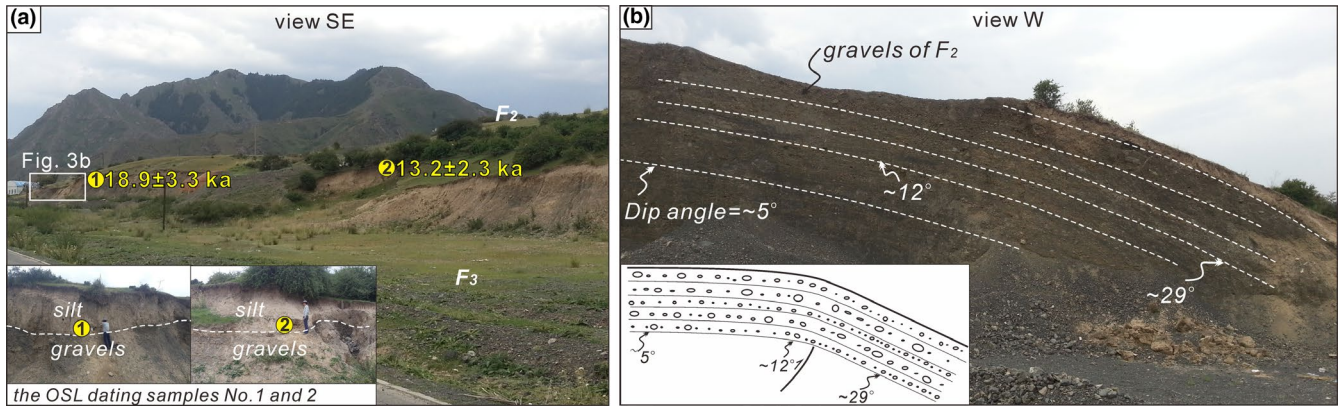


**FIGURE 3** The topographic scarp (a) and the outcrop (b) displaying a systematic change in attitudes in strata at the edge of fan  $F_2$ . These observations are interpreted to indicate thrusting of a blind fault that is the eastern segment of the BF. Yellow circles with numbers show the OSL sampling sites. See Figure 1c for the location of (a). (For interpretation of the references to colour in this figure legend, the reader is referred to the web version of this article.) [Colour figure can be viewed at wileyonlinelibrary.com]

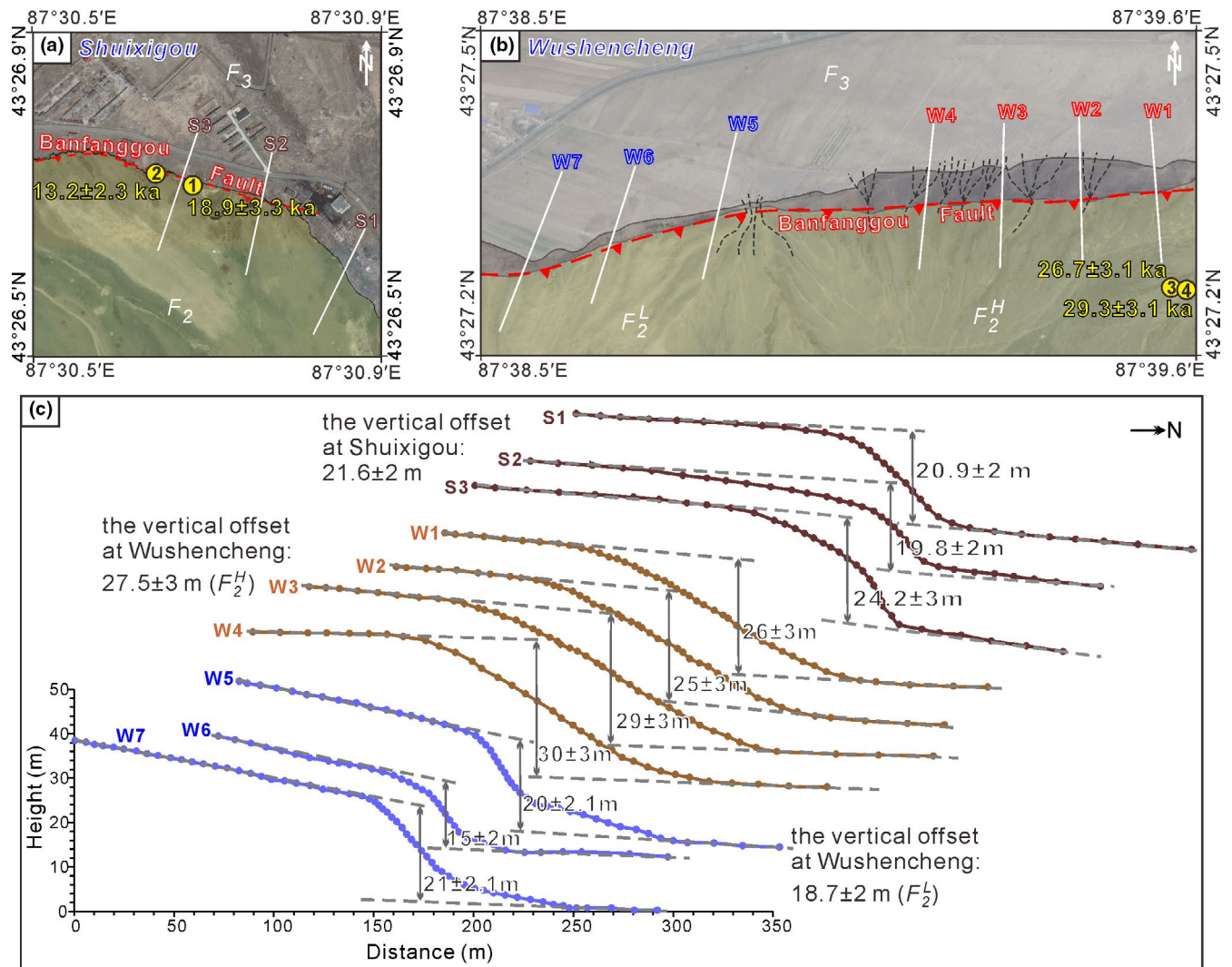


**FIGURE 4** Google Earth images at Shuixigou (a) and Wushencheng (b) and the measured topographic profiles (c) that are used to determine the vertical offset of the Banfanggou fault. Yellow circles with numbers show the OSL sampling sites. (For interpretation of the references to colour in this figure legend, the reader is referred to the web version of this article.) [Colour figure can be viewed at wileyonlinelibrary.com]

that, however, the older terraces have recorded more deformation (Figure S3). In contrast, terrace  $T_4$  is preserved in both the footwall and hanging wall of the BF, and the vertical offset of the BF recorded by this terrace is estimated to be about 20 m. Using the age of ~12 ka estimated by Wu et al. (2020), the average rate of vertical slip on the BF since formation of terrace  $T_4$  is determined to be ~1.7 mm/year.

The more recent thrusting of the BF has been recorded by terrace  $T_1$ . On the east bank of the Urumqi River, the BF reaches the surface between the deposits of terrace  $T_1$  and the underlying Neogene strata (Figure 2b). It has thrust the Neogene mudstone northward onto the Upper Pleistocene conglomerates, and also has offset the surface of terrace  $T_1$ . The measured terrace height profile perpendicular to the thrust scarp indicates that this terrace has been vertically offset about 0.6 m by the BF (Lu et al., 2015). When combined with the abandonment age of 7 ka of terrace  $T_1$ , this vertical offset gives rise to a slip rate of ~0.1 mm/year. In comparison with the rate of 1.7 mm/year constrained by terrace  $T_4$ , this estimated rate is obviously low. The following three reasons may be responsible for this discrepancy. (a) The topographic profile of the Urumqi River terrace  $T_4$  (Lu et al., 2015) was extracted from the DEM comprising 30 m pixels with ~30 m horizontal accuracy and ~20 m vertical accuracy (ASTER GDEM Validation Team, 2009). The low accuracy of the used DEM data may affect the quality of the data (i.e. the offset in this work; Boulton & Stokes, 2018). (b) The  $T_4$  formation age has been estimated from terrace correlation across the northern Chinese Tian Shan foreland (Wu et al., 2020), leading to uncertainty of terrace-abandonment age. (c) The Urumqi River terrace  $T_1$  is currently under farming, and thus the vertical offset of the BF constrained by this terrace is most likely to be underestimated.

#### 4.2.2 | Shuixigou

As shown in section 4.1, thrusting of the BF has caused the systematic changes in attitude of the alluviums of fan  $F_2$  at Shuixigou, and also has formed the fault scarp on the surface of this fan (Figures 3a and 4a). Based on three measured topographic profiles (Figure 4a,c) and the method of Avouac et al. (1993) (Data S1 in Supporting Information for the details), the magnitude of vertical slip on the BF is determined to  $21.6 \pm 2$  m (Figure 4c). Note that the alluviums of fan  $F_3$  have buried the surface of fan  $F_2$  in the footwall of the BF (Figure 4a). Therefore, the vertical offset recorded by fan  $F_2$  at Shuixigou should be greater than the above estimation. Two OSL samples taken from the silt overlying the gravels of fan  $F_2$  are dated to  $18.9 \pm 3.3$  ka and  $13.2 \pm 2.3$  ka respectively (Figure 4a; Table 1). Collectively, these dates suggest a mean abandonment age of fan  $F_2$  to  $16.1 \pm 2$  ka, yielding a minimum estimation of the vertical slip rate of  $1.3 \pm 0.2$  mm/year for the BF.

#### 4.2.3 | Wushencheng

The geomorphological phenomenon here is similar to that at Shuixigou. An obvious topographic scarp exists between fans  $F_2$  and

$F_3$  where the Wushencheng Creek exits from the mountain range (Figures S2b,c). Based on the elevation difference of the fan surface, the fan  $F_2$  at the outlet of the Wushencheng Creek is divided into two secondary surfaces, i.e. the high fan  $F_2^H$  and the low fan  $F_2^L$ . The cumulative vertical offsets of the BF since the abandonment of the  $F_2^H$  and the  $F_2^L$  estimated from the measured topographic profiles are  $27.5 \pm 3$  m and  $18.7 \pm 2$  m, respectively (Figure 4b and c). Considering that the surfaces of these two fans have been buried by the alluviums of  $F_3$  in the footwall of the fault, the above vertical offset of the BF is underestimated. Two OSL samples from the layer of very fine–fine sand in the gravels of fan  $F_2^H$  are dated to  $26.7 \pm 3.1$  ka and  $29.3 \pm 3.1$  ka respectively (Figure 4b; Table 1). Collectively, these dates constrain the abandonment age of fan  $F_2^H$  to  $28 \pm 2.2$  ka, yielding a minimum estimate of the vertical slip rate of  $1.0 \pm 0.1$  mm/year for the BF. No sample was collected from fan  $F_2^L$  owing to lack of suitable outcrops for OSL sampling.

## 5 | DISCUSSION

### 5.1 | Late Quaternary activity of the Banfanggou Fault

Our results show that the western segment of the BF is well exposed (Figure 1c), and that the fault has thrust the Neogene mudstone onto the Quaternary gravels and has deformed the low terraces of the Urumqi River (Figure 2; Figure S3). In contrast, the eastern segment of the BF exists as a blind thrust fault. According to the estimated vertical offset from the Urumqi River terrace  $T_4$  and its abandonment age, the long-term average vertical slip rate over the last 12 kyr is estimated to be ~1.7 mm/year. At Shuixigou and Wushicheng, the vertical slip rates of the eastern segment of the BF during Late Pleistocene are estimated to be 1.3 mm/year and 1.0 mm/year respectively. As mentioned above (Section 4.2), the vertical offsets and thus the vertical slip rates may be underestimated owing to the sedimentation in the footwall of the BF. Overall, the vertical slip rate of the BF during Late Pleistocene is estimated to about 1.0 mm/yr. Despite of some uncertainties deriving from the vertical offset and the geomorphic ages, these resultant vertical slip rates of the BF might imply relatively high seismic risk in the southern margin of the Chaiwopu Basin.

### 5.2 | Spatial pattern of the late Quaternary vertical slip rate in the foreland

In the northern Chinese Tian Shan foreland have developed at least three fold-and-thrust belts (Figure 1b). Previous studies (e.g. Deng et al., 2000; Lu et al., 2019) have shown that the structures of the proximal Belt I have been tectonically inactive during the late Quaternary. The recent deformation in the foreland has been concentrated in the distal structural Belts II and III (e.g. Avouac et al., 1993; Lu et al., 2019; Molnar et al., 1994; Su et al., 2018);

**TABLE 1** Annual doses, equivalent doses and the calculated ages of the OSL dating samples from the fan F<sub>2</sub> in the southern Chaiwopu Basin<sup>a</sup>

Sample No. <sup>b</sup>	Sampled Depth (m)	U (μg/g)	Th (μg/g)	K (%)	Water Content (%)	Environmental Dose Rate (Gy/ka)	Equivalent Doses (Gy)	OSL age (ka) <sup>c</sup>
1	2.3	2.61	11.8	2.06	5.32	4.43	84.07 ± 12.20	18.9 ± 3.3
2	2.4	2.6	10.7	2.15	6.02	4.40	58.08 ± 7.99	13.2 ± 2.3
3	1.5	2.49	8.94	2.32	0.81	4.45	118.83 ± 6.87	26.7 ± 3.1
4	2.5	2.72	9.89	2.12	6.78	4.3	126.08 ± 4.72	29.3 ± 3.1

<sup>a</sup>The dating technique is Simplified Multiple Aliquot Regenerative-dose protocol (SMAR), and the dating material is quartz and the analysed grain size is 4–11 μm.

<sup>b</sup>Locations of the dating samples are shown in Figures 1c, 3, and 4.

<sup>c</sup>The age uncertainty is 1 sigma.

well-developed alluvial sequences preserved where the piedmont rivers flow across these distal structures have thus been faulted and folded. New chronological constraints on abandonment of these alluvial sequences have been reported by recent studies (e.g. Gong et al., 2014, 2015; Lu et al., 2017; Malatesta et al., 2018; Su et al., 2018; Yang et al., 2013). Using the renewed dates available now, here we re-estimate the late Quaternary vertical slip rates of the thrust faults in the northern Tian Shan foreland and further discuss the spatial pattern.

In the structural Belt II exist three E-W-striking thrust faults, i.e. the Huoerguos fault, the Manas fault and the Tugulu fault from west to east (Figure 1b). For the Huoerguos fault, Avouav et al. (1993) and Deng et al. (2000) have estimated the vertical offset of the fault from the Jingou River terrace T<sub>3</sub> to 11.4 m and 6.8–8.2 m respectively. When combined with the terrace abandonment age of 12.6 ± 1.3 ka (Lu et al., 2010), these two vertical offsets give rise to the slip rates of 0.9 mm/year and 0.54–0.65 mm/year, respectively (Table S1). For the Manas fault, the Manas River terrace T<sub>5</sub> has recorded the cumulative vertical offset of 9.2 m (Gong et al., 2015). The OSL dates have constrained the abandonment age of the Manas River terrace T<sub>5</sub> to 5.7–12.4 ka (Gong et al., 2015), yielding the average slip rate of 0.74–1.6 mm/year (Table S1). A similar vertical slip rate of 0.67 mm/year is estimated for the Manas fault from the Manas River terrace T<sub>3</sub> that has recorded the vertical offset of 9.1 m (Deng et al., 2000) over the past 13.5 ka (Gong et al., 2014; Yang et al., 2013). For the Tugulu fault, the terraces of the Taxi and Manas rivers can be used to obtain the deformation rate. At the Taxi River, the formation age of terrace T<sub>3</sub> has been dated at 13.8 ± 0.7 ka (Yuan et al., 2006). When combined with a cumulative vertical offset of ~10.9 m (Deng et al., 2000), this age yields an average rate of 0.79 ± 0.04 mm/year (Table S1). At the Manas river, the formation age of terrace T<sub>3</sub> has been constrained to 13.5 ± 0.6 ka based on the mean ages of the dates from Yang et al. (2013) and Gong et al. (2014). When combined with the vertical offset of ~3.9 m (Deng et al., 2000), an average rate of 0.29 ± 0.01 mm/year is then determined (Table S1). In addition, on the east bank of the Manas River, the vertical offsets recorded by terraces T<sub>5</sub> and T<sub>6</sub> are 4.2 m and 7.8 m (Gong et al., 2015) respectively. When combined with the abandonment

age of each terrace (10.5–12.4 ka and 20 ka), the slip rates are estimated to be ~0.4 mm/year (Table S1).

In the structural Belt III, we focus on the Dushanzi fault and the Halaande fault (Figure 1b). The recent deformation of the Dushanzi fault has been recorded by the Kuitun River terraces. By using the Kuitun River terrace T<sub>2</sub> as the reference, Su et al. (2018) have recently reported a late Quaternary slip rate of ~0.9 mm/year. Then the vertical slip rate is calculated to 0.67 ± 0.14 mm/year by using a fault dip of 50° (Table S1). A relatively low slip rate of 0.45 mm/year (Table S1) is calculated from the Kuitun River terrace T<sub>3</sub> having the abandonment age of 13 ka (Malatesta et al., 2018) and recording the vertical offset of ~6 m (Deng et al., 2000). The Halaande fault has caused the fault scarp with the vertical offset of 3.2 m on the young terraces of the Telikengsa River (the ancient Anjihai River; Deng et al., 2000; Lu et al., 2017). Lu et al. (2017) have constrained the formation age of the youngest terrace to 3.6 ka by OSL dating, yielding a vertical slip rate of 0.89 mm/year (Table S1).

Most of the above estimations of the late Quaternary vertical slip rates of the thrust faults in the structural Belts II and III, northern Chinese Tian Shan foreland cluster around 0.4–0.9 mm/year (Table S1), likely implying uniform thrusting on most of the thrust faults across the foreland. In the eastern part of the foreland, however, the BF in the southern margin of Chaiwopu Basin may have a relatively high vertical slip rate of likely >1 mm/year. Note that uncertainty exists on the slip rate of the BF presented in this work. Better estimations of the deformation rate of the BF need more numerical dates on abandonment of geomorphic surfaces and better determinations of the vertical offset.

## 6 | CONCLUSIONS

This work characterizes the late Quaternary activation of the Banfanggou fault (BF) in the southern margin of the Chaiwopu Basin, northern Chinese Tian Shan foreland by the fluvial geomorphological investigations. At the Urumqi River, the BF, dipping south with an angle of 60–80°, has thrust the Neogene mudstone onto the Quaternary gravels and has displaced the surfaces of river terraces. In contrast, the BF exists as a blind thrust fault in the eastern part

of the southern margin of the basin. The vertical offset recorded by the Urumqi River terrace  $T_4$  is determined to ~20 m based on the extracted topographic profile from the DEM. Based on the abandonment age of 12 ka derived from regional geomorphic correlation, a long-term average vertical slip rate of 1.7 mm/year is estimated. At Shuixigou and Wushencheng in the eastern part of the southern margin of the Chaiwopu Basin, the vertical slip rates of the BF are determined to 1.3 mm/year and 1.0 mm/year respectively. Better estimations of the vertical slip rate of the BF need more numerical dates on abandonment of geomorphic surfaces and better determinations of the vertical offset. Using the renewed geomorphic ages reported by the recent studies, the vertical slip rates on most of the thrust faults in the western part of the northern Chinese Tian Shan foreland are re-estimated to be 0.4–0.9 mm/year, likely implying uniform thrusting across the foreland.

#### ACKNOWLEDGEMENTS

This study is financially supported by the National Natural Science Foundation of China (Grant Nos. 41771013 and 41371031) and the Fundamental Research Funds for the Central Universities. Zhen Wang and Tianqi Zhang are especially appreciated for their field assistance. Three reviewers and the guest editor Professor Yuntao Tian are greatly appreciated for their constructive comments on the manuscript, which resulted in the great improvement of the manuscript.

#### CONFLICT OF INTEREST

The authors declare that they have no any conflict of interest about this work.

#### DATA AVAILABILITY STATEMENT

The data used in this study are available in the document "Supplementary information.docx" uploaded online.

#### REFERENCES

- ASTER GDEM Validation Team. (2009). ASTER GDEM Validation Summary Report.
- Avouac, J.-P., & Tapponnier, P. (1993). Kinematic model of active deformation in central Asia. *Geophysical Research Letters*, 20(10), 895–898. <https://doi.org/10.1029/93gl00128>
- Avouac, J.-P., Tapponnier, P., Bai, P., You, M., & Wang, G. (1993). Active thrusting and folding along the northern Tien Shan and late Cenozoic rotation of the Tarim relative to Dzungaria and Kazakhstan. *Journal of Geophysical Research*, 98(B4), 6755–6804. <https://doi.org/10.1029/92jb01963>
- Boulton, S. J., & Stokes, M. (2018). Which DEM is best for analyzing fluvial landscape development in mountainous terrains? *Geomorphology*, 310, 168–187. <https://doi.org/10.1016/j.geomorph.2018.03.002>
- Burchfiel, B. C., Brown, E. T., Deng, Q., Feng, X., Li, J., Molnar, P., Shi, J., Wu, Z., & You, H. (1999). Crustal shortening on the margins of the Tien Shan, Xinjiang, China. *International Geological Review*, 41(8), 665–700. <https://doi.org/10.1080/00206819909465164>
- Charreau, J., Avouac, J.-P., Chen, Y., Dominguez, S., & Gilder, S. (2008). Miocene to present kinematics of fault-bend folding across the Huoerguosi anticline, northern Tianshan (China), derived from structural, seismic, and magnetostratigraphic data. *Geology*, 36(11), 871–874. <https://doi.org/10.1130/G25073A.1>
- Charreau, J., Saint-Carlier, D., Lavé, J., Dominguez, S., Blard, P.-H., Avouac, J.-P., Brown, N. D., Malatesta, L. C., Wang, S. L., & Rhodes, E. J. (2018). Late Pleistocene acceleration of deformation across the northern Tianshan piedmont (China) evidenced from the morpho-tectonic evolution of the Dushanzi anticline. *Tectonophysics*, 730, 132–140. <https://doi.org/10.1016/j.tecto.2018.02.016>
- Deng, Q. D., Feng, X. Y., Zhang, P. Z., Xu, X. W., Yang, X. P., Peng, S. Z., & Li, J. (2000). *Active Tectonics of the Tian Shan Mountains*. Seismology Press. (in Chinese with English abstract).
- Fu, X., Li, S. H., Li, B., & Fu, B. H. (2017). A fluvial terrace record of late Quaternary folding rate of the Anjihai anticline in the northern piedmont of Tian Shan, China. *Geomorphology*, 278, 91–104. <https://doi.org/10.1016/j.geomorph.2016.10.034>
- Gao, C. H. (2004). Sedimentary facies changes and climatic-tectonic controls in a foreland basin, the Urumqi River, Tian Shan, Northwest China. *Sedimentary Geology*, 169, 29–46. <https://doi.org/10.1016/j.sedgeo.2004.04.006>
- Gong, Z. J., Li, S. H., & Li, B. (2014). The evolution of a terrace sequence along the Manas River in the northern foreland basin of Tian Shan, China, as inferred from optical dating. *Geomorphology*, 213, 201–212. <https://doi.org/10.1016/j.geomorph.2014.01.009>
- Gong, Z. J., Li, S. H., & Li, B. (2015). Late Quaternary faulting on the Manas and Hutubi reverse faults in the northern foreland basin of Tian Shan, China. *Earth and Planetary Science Letters*, 424, 212–225. <https://doi.org/10.1016/j.epsl.2015.05.030>
- Li, Y. L., Si, S. P., Lu, S. H., & Wang, Y. R. (2012). Tectonic and climatic controls on the development of the Kuitun River terraces in the northern piedmont of Tianshan Mountains. *Quaternary Sciences*, 32(5), 880–890. (in Chinese with English abstract).
- Liu, L. J., & Chen, W. (2002). Geometric and kinematic characteristic of thick skinned and thin skinned nappe structures in the northern Tian Shan (in Chinese, with English abstract). *Natural Gas Industry*, 22(5), 104–105. (in Chinese with English abstract).
- Lu, H. H., Burbank, D. W., & Li, Y. L. (2010). Alluvial sequence in the north piedmont of the Chinese Tian Shan over the past 550 kyr and its relationship to climate change. *Palaeogeography, Palaeoclimatology, Palaeoecology*, 285(3–4), 343–353. <https://doi.org/10.1016/j.palaeo.2009.11.031>
- Lu, H., Li, B., Wu, D., Zhao, J., Zheng, X., Xiong, J., & Li, Y. (2019). Spatiotemporal patterns of the Late Quaternary deformation across the northern Chinese Tian Shan foreland. *Earth-Science Reviews*, 194, 19–37. <https://doi.org/10.1016/j.earscirev.2019.04.026>
- Lu, H. H., Wang, Z., Zhang, T. Q., Zhao, J. X., Zheng, X. M., & Li, Y. L. (2015). Latest Miocene to Quaternary deformation in the southern Chaiwopu Basin, northern Chinese Tian Shan foreland. *Journal of Geophysical Research*, 120(12), 8656–8671. <https://doi.org/10.1002/2015JB012135>
- Lu, H. H., Wu, D. Y., Cheng, L., Zhang, T. Q., Xiong, J. G., Zheng, X. M., & Li, Y. L. (2017). Late Quaternary drainage evolution in response to fold growth in the northern Chinese Tian Shan foreland. *Geomorphology*, 299, 12–23. <https://doi.org/10.1016/j.geomorph.2017.09.037>
- Lu, H. H., Xu, Y. D., Niu, Y., Wang, Z., Wang, H., Zhao, J. X., Zhang, W. G., & Zheng, X. M. (2016). Late Quaternary loess deposition in the southern Chaiwopu Basin of the northern Chinese Tian Shan foreland and its palaeoclimatic implications. *Boreas*, 45, 304–321. <https://doi.org/10.1111/bor.12152>. ISSN 0300-9483
- Lu, H. H., Zhang, T. Q., Zhao, J. X., Si, S. P., Wang, H., Chen, S. J., Zheng, X. M., & Li, Y. L. (2014). Late Quaternary alluvial sequence and uplift-driven incision of the Urumqi River in the north front of the Tian Shan, northwestern China. *Geomorphology*, 219, 141–151. <https://doi.org/10.1016/j.geomorph.2014.05.001>
- Malatesta, L. C., Avouac, J.-P., Brown, N. D., Breitenbach, S. F. M., Pan, J. W., Chevalier, M.-L., Rhodes, E., Saint-Carlier, D., Zhang, W. J., Charreau, J., Lavé, J., & Blard, P.-H. (2018). Lag and mixing during sediment transfer across the Tian Shan piedmont caused by

- climate-driven aggradation-incision cycles. *Basin Research*, 30, 613–635. <https://doi.org/10.1111/bre.12267>
- Molnar, P., Brown, E. T., Burchfiel, B. C., Deng, Q. D., Feng, X. Y., Li, J., Raisbeck, G. M., Shi, J. B., Wu, Z. M., Yiou, F., & You, H. C. (1994). Quaternary climate change and the formation of river terraces across growing anticlines on the north flank of the Tianshan, China. *Journal of Geology*, 102, 583–602. <https://doi.org/10.2307/30068558>
- Najman, Y., Pringle, M., Godin, L., & Oliver, G. (2001). Dating of the oldest continental sediments from the Himalayan foreland basin. *Nature*, 410, 194–197. <https://doi.org/10.1038/35065577>
- Qiu, J. H., Rao, G., Wang, X., Yang, D. S., & Xiao, L. X. (2019). Effects of fault slip distribution on the geometry and kinematics of the southern Junggar fold-and-thrust belt, northern Tian Shan. *Tectonophysics*, 772, 209–228. <https://doi.org/10.1016/j.tecto.2019.228209>
- Reigber, C. H., Michel, G. W., Galas, R., Angermann, D., Klotz, J., Chen, J. Y., Papschev, A., Arslanov, R., Tzurkov, V. E., & Ishanov, M. C. (2001). New space geodetic constraints on the distribution of deformation in Central Asia. *Earth and Planetary Science Letters*, 191(1–2), 157–165. [https://doi.org/10.1016/S0012-821X\(01\)00414-9](https://doi.org/10.1016/S0012-821X(01)00414-9)
- Scharer, K. M., Burbank, D. W., Chen, J., & Weldon II, R. (2006). Kinematic models of fluvial terraces over active detachment folds: Constraints on the growth mechanism of the Kashi-Atushi fold system, Chinese Tian Shan. *Geological Society of America Bulletin*, 118, 1006–1021. <https://doi.org/10.1130/B25835>
- Su, P., He, H. L., Wei, Z. Y., Lu, R. Q., Shi, F., Sun, H. Y., Tan, X. B., & Hao, H. J. (2018). A new shortening rate across the Dushanzi anticline in the northern Tian Shan Mountains, China from lidar data and a seismic reflection profile. *Journal of Asian Earth Sciences*, 163, 131–141. <https://doi.org/10.1016/j.jseaes.2018.06.008>
- Tapponnier, P., Xu, Z., Roger, F., Meyer, B., Arnaud, N., Wittlinger, G., & Yang, J. (2001). Oblique stepwise rise and growth of the Tibetan Plateau. *Science*, 294(5547), 1671–1677. <https://doi.org/10.1126/science.105978>
- Wei, Z. Y., He, H. L., Su, P., Zhuang, Q. T., & Sun, W. (2019). Investigating paleoseismicity using fault scarp morphology of the Dushanzi Reverse Fault in the northern Tian Shan, China. *Geomorphology*, 327, 542–553. <https://doi.org/10.1016/j.jsg.2020.103990>
- Wu, D. Y., Li, B. J., Lu, H. H., Zhao, J. X., Zheng, X. M., & Li, Y. L. (2020). Spatial variations of river incision rate in the northern Chinese Tian Shan range derived from late Quaternary fluvial terraces. *Global and Planetary Change*, 185, <https://doi.org/10.1016/j.gloplacha.2019.103082>
- Yang, S., Jie, L. I., & Qi, W. (2008). The deformation pattern and fault rate in the Tian Shan Mountains inferred from GPS observations. *Science in China Series D: Earth Sciences*, 51, 1064–1080. <https://doi.org/10.1007/s11430-008-0090-8>
- Yang, X. P., Li, A., & Huang, W. L. (2013). Uplift differential of active fold zones during the late Quaternary, northern piedmonts of the Tianshan Mountains, China. *Science China Earth Science*, 56(5), 794–805. <https://doi.org/10.1007/s11430-012-4531-z>
- Yuan, Q. D., Guo, Z. J., Zhang, Z. C., Wu, C. D., & Fang, S. H. (2006). The late Cenozoic deformation of terraces on the north flank of Tian Shan Mountains and the tectonic evolution (in Chinese with English abstract). *Acta Geologica Sinica*, 80(2), 210–216. (in Chinese with English abstract)
- Zhang, P. Z. (2004). Late Cenozoic tectonic deformation in the Tianshan Mountain and its foreland basins. *Chinese Science Bulletin*, 49(4), 311–313. <https://doi.org/10.1360/03wd0488>
- Zhou, S. Z., Jiao, K. Q., Zhao, J. D., Zhang, S. Q., Cui, J. X., & Xu, L. B. (2002). Geomorphology of the Ürümqi River Valley and Quaternary uplift of Tianshan Mountains in Quaternary. *Science in China (Series D: Earth Science)*, 45(11), 961–968. <https://doi.org/10.3969/j.issn.1674-7313.2002.11.001>

## SUPPORTING INFORMATION

Additional supporting information may be found online in the Supporting Information section.

Data S1. Supplementary information about OSL dating and topographic profiles across the fault scarps.

**How to cite this article:** Pang L, Cheng L, Lu H, Guan X, Wu D, Zheng X. Late Quaternary thrusting in the southern margin of the Chaiwopu Basin, northern Chinese Tian Shan foreland. *Terra Nova*. 2021;33:159–167. <https://doi.org/10.1111/ter.12501>